Queue estimation in a connected vehicle environment
A convex approach

Author(s):
Yang, Kaidi (iD); Menendez, Monica

Queue Estimation in a Connected Vehicle Environment: A Convex Approach

Kaidi Yang and Monica Menendez

Abstract—This paper proposes a convex optimization based algorithm for queue profile estimation in a connected vehicle environment, which can also be used for trajectory reconstruction, delay evaluation, etc. This algorithm generalizes the widely-adopted assumption of a linear back of queue (BoQ) curve to a piecewise linear BoQ curve to consider more practical scenarios. The piecewise linear BoQ curve is estimated via a convex optimization model, ensuring efficient computation. Moreover, this paper explicitly handles cases with low penetration rates and low sampling rates, as well as measurement noises. Additionally, the proposed methodology is extended to an urban arterial, reusing the estimated departure information from the upstream intersections to further improve the estimation accuracy. Finally, two online implementation approaches are presented to perform real-time queue estimation.

The proposed methodology is tested with two datasets: the Lankershim dataset in the NGSIM project and the simulated dataset of Wehntalerstrasse, Zurich, Switzerland. Results show that the error is less than 1.5 cars in undersaturated scenarios and 5.2 cars in oversaturated scenarios if the penetration rates are larger than 0.1 and sampling rates are higher than $0.05\mathrm{s}^{-1}$. It is demonstrated that by considering a piecewise linear BoQ curve, the estimation accuracy can be improved by up to 16%. Incorporating flow successfully can also reduce the estimation error by up to 16%. Results further show that the proposed methodology is robust to measurement errors. It is finally shown that the proposed framework can be solved within a reasonable time (0.8s), which is sufficient for most real-time applications.

Index Terms—queue length estimation, connected vehicle technology, kinematic wave theory, piecewise linear regression, trajectory reconstruction

I. INTRODUCTION

QUEUE estimation is crucial for intelligent transportation systems. In urban traffic networks, queue lengths are an essential input to adaptive signal control strategies [1]–[8] and performance measurements at signalized intersections or arterials [9].

Traditionally, queue length estimation uses information from roadside detectors, e.g. loop detectors [10], cameras [11], and event-based data (including both vehicle-detector actuation events and signal phase change events) [12]. Although roadside detectors provide aggregated traffic information such as density, flow and speed, they are installed at fixed locations, suffering from limited information coverage and extra cost for installation and maintenance.

Kaidi Yang is with the Traffic Engineering Group, Institute for Transport Planning and Systems, ETH Zurich, Switzerland (e-mail: kaidi.yang@ivt.baug.ethz.ch); Monica Menendez is with Division of Engineering, New York University Abu Dhabi, UAE (email: monica.menendez@nyu.edu)

Recently, the emerging connected vehicle technology is attracting increasing attention as an alternative to traditional traffic detectors. Equipped with Global Positioning System (GPS) devices and wireless communication systems, connected vehicles are capable of reporting real-time information (e.g. position, speed, acceleration rate and direction) to each other (vehicle to vehicle, V2V) or to the roadside infrastructure (vehicle to infrastructure, V2I), providing a better spatial coverage of information [13], [14].

One challenge on queue length estimation using this technology is the penetration rate, which is expected to remain low in the near future. The penetration rate highly influences the estimation accuracy, as only equipped vehicles can report information. Another challenge is the sampling rate, i.e. the frequency a vehicle reports information, which can also be calculated as the inverse of the time interval between two consecutive reports. Some of the existing literature requires that the equipped vehicles report information every second [15]–[17]. However, the sampling rate could be lower in reality due to the transmission and storage capacity. Moreover, the obtained information can also be noisy, as there might be communication latency, data corruption, or GPS noises. Therefore, the proposed algorithm should be robust enough to handle these challenges.

The existing literature on queue length estimation can be mostly classified into two categories. The first category uses queuing theory, usually with stochastic arrivals. For example, the authors in [18]–[20] proposed a probabilistic model to estimate the expected queue length, assuming a Poisson arrival process of vehicles and a Bernoulli distribution for whether a vehicle is equipped or not. [21] uses a stochastic gradient descent method and a queuing diagram to estimate the queue lengths. However, these works assumed point queues, and did not consider the spatial traffic dynamics (e.g. the propagation of traffic waves).

The second category is based on Lighthill-Whitham-Richards (LWR) kinematic wave theory [22]–[24]. Some works use the sampled travel time obtained from the trajectory data to estimate the queue length (e.g. [25]–[29]). [25] and [26] fitted the queue curves based on the observation of a decreasing delay pattern. A support vector machine (SVM) based method is proposed in [27] to identify the critical points for the new cycle based on delay and travel time. [28] and [29] considered the acceleration and deceleration process to calculate the queue location in the discharging process and to reconstruct the long queue when spillbacks happen, respectively. Other works directly use the trajectory data to estimate the piecewise linear back of queue (BoQ) that consists

of a series of shockwaves. Through the BoQ curve, not only queue length and platoons, but also traffic flow, density, and even trajectories can be recovered. The estimation of the BoQ curve can be formulated into a regression and/or classification problem. The general process for estimating the BoQ curve follows two steps. In the first step, critical points where the traffic states change are identified on the time-space diagram. Each critical point is a two dimensional vector: time t and location x. There are a few different definitions of critical points. [15] estimated the critical points as the first trajectory points with speed lower than a threshold; [30] and [31] fitted the vehicle trajectory into a piece-wise linear function, and identified the critical points as the intersection between each two pieces; [32] determined the critical points using both speed and acceleration information; [33] defined the critical points as the first calculated x-t point with zero speed. In contrast with the existing research, and in order to retrieve flow information from the shockwaves, this paper proposes another way to retrieve the critical points that is coherent with the kinematic wave theory. In the second step, the existing literature has obtained the BoQ curve from the critical points using variational theory [15], [34], fundamental diagram [31], linear regression [30], [32], or piecewise linear fitting [33].

Although the algorithms developed in the aforementioned works perform well, there is still room for improvement. For example, most of the aforementioned works, e.g. [25]–[30] and [32], relied on the assumption of constant arrival rate (thus a linear BoQ curve) in each signal cycle. However, such assumption cannot capture the variation in demand. In an arterial, for example, the arrival rate to the downstream intersection may be affected by the signal timings of the upstream intersection, and thus is varying. In such cases, relaxing the assumption of a linear BoQ curve may yield better results. Some of the other works, e.g. [15], [33] and [34] aimed to estimate a non-linear BoQ and proposed complex non-convex models, which can be time consuming to find the global optimum. [31] directly obtained the shockwave for each trajectory point using the fundamental diagram, which works for very low penetration rates, but might be sensitive to GPS noises. Furthermore, none of these works explore the queue estimation in an arterial. The discharging process of the upstream intersection provides additional flow information that can be utilized to improve the accuracy of the queue estimation. Finally, most of these works focus on the queue estimation of undersaturated scenarios, whereas for the purpose of traffic control, oversaturated scenarios are of more significance.

To solve the above mentioned problems, this paper proposes a queue estimation method using connected vehicle information based on the work of [33]. The contributions of this paper are four-fold.

1) We relax the assumption of a constant arrival rate by estimating a piecewise linear BoQ curve with a convex optimization model. The methodology proposed in this paper is independent of the demand, hence it can handle any demand distribution (known or not). The convexity of the proposed model guarantees a low computational cost in the BoQ estimation.

2) The proposed convex model is further extended to estimate queue lengths in arterials. We propose a new framework to reuse the information on the estimated discharging flow at the upstream intersections to improve the estimation accuracy, especially if the penetration rate is low. The effects of platoon dispersion are also considered. The proposed framework does not require the tracking of vehicles, which helps protect privacy.

3) We explicitly handle scenarios with low data quality. On one hand, an alternative method is proposed to deal with the cases with low sampling rates and low penetration rates by using the acceleration and deceleration information. On the other hand, the determination of the critical points and the BoQ/FoQ(front of queue) curves is based on the whole dataset, which makes the method more robust to measurement noises.

4) The proposed method is of pragmatic significance. First, it is able to work in both undersaturated and oversaturated scenarios. Second, we propose an online implementation framework, which is both accurate and computationally efficient.

The paper is organized as follows. The convex formulation for the queue estimation for a single signalized intersection is proposed in Section II. Section III utilizes the arterial level data to further improve the accuracy of the queue estimation. Section IV adapts the proposed method to handle the cases with limited data. Section V describes the simulations settings, and Section VI shows the queue estimation results on the Next Generation Simulation (NGSIM) dataset [35] and the simulated dataset of an arterial of Wehntalerstrasse, Zurich, Switzerland. A sensitivity analysis is performed in Section VII. Section VIII studies the online implementation of the methodology, and Section IX concludes the paper.

II. GENERAL METHODOLOGY

This section proposes a general methodology for queue estimation at a signalized intersection using connected vehicle technology. For the reader's convenience, a list of the most important variables is given in Table 1.

The signal timing plan can be either fixed, actuated or adaptive. In this paper, it is assumed that the signal timings are available, i.e. the start of the red signal, r_p, and the start of the green signal, g_p, are available for each cycle p. This assumption can be relaxed, however, with classification methods (e.g. [27]) or clustering methods (e.g. [33]).

The fundamental diagram of the link is assumed to be triangular with known parameters (free flow speed, jam density, backward wave speed). In practice, the shape and parameters of the fundamental diagram can be calibrated using trajectory data (see [36]).

A certain percentage of vehicles are assumed to be equipped with connected vehicle technology (GPS sensors and V2I communication devices). It is assumed that these vehicles are able to communicate with the intersection controller if they are within a certain radius of it. This radius is upper bounded by the physical limit of the communication range and the length of the links (as otherwise route choice of the vehicles will

TABLE I
NOMENCLATURE.

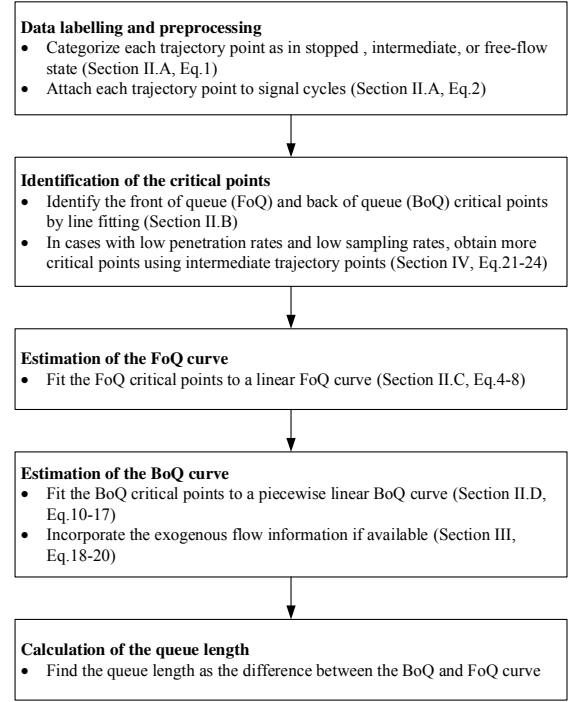|	
M	set of all equipped vehicles, indexed by m;
J	set of all trajectory points, indexed by j;
P	set of signal cycles, indexed by p;
V	set of all trajectory points classified as in the free flow state;
S	set of all trajectory points classified as in the stopped state;
I	set of all trajectory points classified as in the intermediate state;
J_m	set of trajectory points associated to vehicle m;
V_p	set of trajectory points classified as in the free flow state for cycle p;
S_p	set of trajectory points classified as in the stopped state for cycle p;
I_p	set of trajectory points classified as in the intermediate state for cycle p;
A_p	set of trajectory points classified as in the accelerating state for cycle p;
D_p	set of trajectory points classified as in the decelerating state for cycle p;
B_p	set of BoQ critical points for cycle p;
F_p	set of FoQ critical points for cycle p;
r_p	start of the red signal in cycle p;
g_p	start of the green signal in cycle p;
$\underline{u}$	low speed threshold to detect stopped trajectory points;
$\bar{u}$	high speed threshold to detect free-flow trajectory points;
k_{jam}	jam density on the link;
u_f	free flow speed on the link;
w	absolute value of the backward wave speed on the link;
x_j	location coordinate of trajectory point j;
t_j	time coordinate of trajectory point j;
v_j	speed coordinate of trajectory point j;
T_{step}	time step for the back of queue estimation;
α_i	slope of the back of queue curve at the ith time step;
π_i	time of the ith time step for the BoQ curve estimation.

Fig. 1. Flowchart of the proposed general methodology.

IV, respectively. An illustration of the process is given in Fig.2.
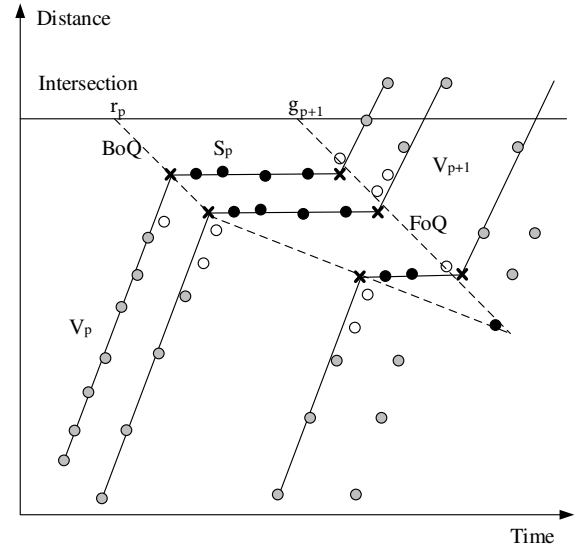

Fig. 2. Illustration of the method. The gray dots are marked as free-flow, the white dots are in the intermediate state, the black dots are stopped. The points with cross marks represent the critical points. The solid lines represent the reconstructed theoretical trajectories; the dashed lines represent the front of queue (FoQ) curve and the back of queue (BoQ) curve.

be needed). Recent technologies, e.g. Dedicated Short Range Communications (DSRC), can provide a communication range of up to 1000 meters [37]. Therefore, for simplicity, this radius is assumed to be comparable with the length of a typical link. The equipped vehicles send trajectory information (time, location and speed) to the controller at some sampling rates, which do not have to be constant for each trajectory, and do not need to be synchronized in time.

In this section, it is assumed that there is at least one stopped trajectory point and one moving trajectory point for each equipped vehicle. This assumption is made for presentation simplicity here, and will be relaxed in Section IV.

The set of trajectory points is defined as J. The trajectory information is defined as a vector (t_j, x_j, v_j), where the three coordinates represent current time, location, and speed, respectively. In this paper, the location of a vehicle j, x_j, is assumed to be 0 at the intersection, and a negative value if the vehicle is on the upstream link of the intersection.

Fig.1 shows the flowchart of this methodology. Given a set of trajectory points, the method estimates the queue length in five steps: 1) data labelling and preprocessing; 2) identification of the critical points; 3) estimation of the FoQ curve; 4) estimation of the BoQ curve; and 5) calculation of the queue length. The rest of this section presents the main parts of the five steps in detail. The other parts, i.e. incorporating the flow information for BoQ estimation and including the intermediate states, will be presented in Section III and Section

A. Data labelling and preprocessing

In this step, the trajectory points will be labelled as in a stopped state, free-flow state, or intermediate state, and then attached to each signal cycle.

A trajectory point is identified as stopped if the speed is lower than a critical value $\underline{u}$, and free-flow if the speed is higher than a critical value $\bar{u} > \underline{u}$. Define set S as the set of all trajectory points in the stopped state, set V as the set of all trajectory points in the free-flow state. The other trajectory points are identified as in the intermediate state (i.e. accelerating/decelerating state), denoted as set I. This can be summarized as

$$j \in \begin{cases} S, & \text{if } v_j \leq \underline{u} \\ I, & \text{if } \underline{u} < v_j \leq \bar{u} \\ V, & \text{if } v_j > \bar{u} \end{cases} \tag{1}$$

In this section, intermediate trajectory points are not considered for simplicity. However, these trajectory points can be useful if there are no stopped or free-flow trajectory points for an equipped vehicle trajectory, which will be discussed in Section IV.

Each trajectory point (stopped, free-flow, or intermediate) is attached to a signal cycle. This can be described in Eq.(2). Note that different trajectory points of a vehicle may be attached to different cycles, if this vehicle queues for multiple cycles.

$$j \in \begin{cases} V_p, & \text{if } g_p \leq x_j/w + t_j < g_{p+1} \text{ and } j \in V \\ I_p, & \text{if } g_p \leq x_j/w + t_j < g_{p+1} \text{ and } j \in I \\ S_p, & \text{if } g_p \leq x_j/w + t_j < g_{p+1} \text{ and } j \in S \end{cases} \tag{2}$$

where V_p, I_p and S_p represent the set of free-flow, intermediate, and stopped trajectory points in a signal cycle, respectively.

B. Identification of the critical points

Critical points represent the transition between two traffic states. As is shown in Fig.2, the FoQ critical points separate the stopped state in cycle p and the free-flow state in cycle $p + 1$, and represents the time and location where a vehicle starts to be discharged. The BoQ critical points separate the free-flow state in cycle p to the stopped state in cycle p, and represents the process where a vehicle comes to a stop.

Let J_m be the trajectory points reported by the equipped vehicle m. Then for cycle p, the set $J_m \cap V_p$ represents the free-flow trajectory points of equipped vehicle m in this cycle; the set $J_m \cap S_p$ represents the stopped trajectory points of equipped vehicle m in this cycle.

The FoQ critical point for trajectory m in signal cycle p can be calculated as the intersect between the lines formed by trajectory points in $J_m \cap S_p$ (the stopped points for trajectory m in signal cycle p) with a slope of 0 and $J_m \cap V_{p+1}$ (the moving points for trajectory m in signal cycle $p + 1$) with a slope of u_f. Both lines can be derived using linear regression, and the critical points can be identified by solving the linear equations. Denote the set of FoQ critical points in cycle p as F_p.

For trajectory m and signal cycle p, each BoQ critical point is determined as the intersect between two lines: 1) the line fitted on set $J_m \cap V_p$ (the moving points of vehicle m for trajectory in signal cycle p) with a slope of u_f; and 2) the

line fitted on set $J_m \cap S_p$ (the stopped points of vehicle m for trajectory in signal cycle p) with a slope of 0. Denote the set of BoQ critical points in cycle p as B_p.

This definition of the critical points approximates each vehicle trajectory as a piecewise linear curve of stopped segments and free-flow segments. This is consistent with the kinematic wave theory with the assumption of a triangular fundamental diagram. This approximation is also invariant with respect to vehicle delay.

C. Estimation of the FoQ curve

As is shown in Fig.2, the FoQ curve between cycles p and $p + 1$ is the discharging line in cycle p. It is a straight line that i) separates the stopped trajectory points in cycle p, S_p, and the free-flow trajectory points in cycle $p + 1$, V_{p+1}; ii) crosses the critical points in set F_p between S_p and V_{p+1}; iii) has a slope of $-w$, where w is the absolute value of the backward wave speed.

Denote the FoQ curve as a line on the $x-t$ plane represented by

$$x + wt - h = 0 \tag{3}$$

where h is the decision variable, representing the intercept on the distance axis, x. Then estimating the FoQ curve is equivalent to determining the intercept h that satisfies the criteria listed above.

Hence, the problem of estimating FoQ can be formulated into the following optimization model Eq.(4)-Eq.(8).

$$\min \sum_{j \in F_p} \epsilon_j^2 + \lambda_1 \sum_{j \in S_p} e_j + \lambda_2 \sum_{j \in V_{p+1}} e_j \tag{4}$$

$$\text{s.t. } x_j + wt_j - h = \epsilon_j, \ j \in F_p \tag{5}$$

$$x_j + wt_j - h \leq e_j, \ j \in S_p \tag{6}$$

$$x_j + wt_j - h \geq -e_j, \ j \in V_{p+1} \tag{7}$$

$$e_j \geq 0, \ j \in V_{p+1} \cup S_p \tag{8}$$

where the decision variable is the intercept h. Constraint Eq.(5) defines the error of fitting the critical points with Eq.(3); Eq.(6) and Eq.(7) guarantee that the discharging line separates the stopped and moving states. The slack variables e_j are introduced to handle the case where the stopped state and the free flow state are not strictly separable by straight lines. This could happen in scenarios with multiple lanes, or with large measurement errors. The objective function Eq.(4) minimizes the summed square fitting errors and classification errors. λ_1 and λ_2 are regularization factors that control the weight of the the classification errors. If λ_1 and λ_2 are small, the model gives more emphasis to fitting than to classification. Besides, if $\lambda_1 > \lambda_2$, the model focuses more on the stopped state.

The optimization model Eq.(4)-Eq.(8) is convex, which can be solved in polynomial time with the inner point method or Newton's method. Solving this model gives the discharging line (i.e., FoQ curve) $x + wt - h = 0$.

Note that the formulation Eq.(4)-Eq.(8) relies on the underlying assumption that there is at least one FoQ critical point. In other words, it is assumed in this section that there exists

at least one vehicle m such that both $V_{p+1} \cap J_m$ and $S_p \cap J_m$ are not empty. This assumption will be relaxed in Section IV.

D. Estimation of the BoQ curve

According to LWR theory, the BoQ curve is modelled as a piecewise linear curve $x = x(t)$ that crosses the critical points in set B_p and separates the moving state V_p and the stopped state S_p (see Fig.2). All the trajectory points in V_p should be below the BoQ curve, and all the trajectory points in S_p should be above the BoQ curve.

The estimation of the BoQ curve can be formulated as a classification problem with a piecewise linear boundary. In this paper, the piecewise linear boundary is determined using the method proposed in [38]. The key idea of this model is to divide the region of interest into some subregions and find a classification line in each region through a global optimization model. For the BoQ curve estimation problem, the region of interest Π is chosen as the time period between the start time of a cycle to the time when the queue is cleared. The BoQ curve begins from the start time of the red signal in cycle p, r_p. The time when the BoQ curve ends (the queue is cleared) is generally unknown. It can be chosen as a time sufficiently large. For real-time queue estimation, the end time of the region can be the current time. Then the region of interest is divided into time intervals $\Pi_i = \{j | \pi_i \leq t_j < \pi_{i+1}\}$, $i = 1, \cdots, n$, where π_1 is the start time of Π and π_{n+1} is the end time of Π. The length of each time interval $T_{\text{step}} = \pi_{i+1} - \pi_i$ determines the precision of the BoQ curve. If this size is too large, it might give an inaccurate BoQ. If this size is too small, it might lead to over-fitting. A sensitivity analysis on the time interval length is conducted in Section VII.

In this way, the BoQ curve represented by a continuous piecewise linear curve $BoQ(t)$ on the $x - t$ plane can be written as

$$x(t) = BoQ(t) = \begin{cases} \alpha_1 t + \beta_1, & \pi_1 \leq t < \pi_2 \\ \cdots \\ \alpha_n t + \beta_n, & t \geq \pi_n \end{cases} \quad (9)$$

where $\alpha_i, \beta_i, i = 1, \cdots, n$ are the slopes and intercepts in each time interval.

The estimation of the BoQ curve can be modelled as

$$\min \frac{1}{2} \sum_{j \in B_p} \epsilon_j^2 + \lambda_1 \sum_{j \in S_p} e_j + \lambda_2 \sum_{j \in V_p} e_j + \lambda_3 \sum_{i=2}^{n} |\alpha_i - \alpha_{i-1}| \quad (10)$$

$$\text{s.t. } \alpha_{i-1} \pi_i + \beta_{i-1} = \alpha_i \pi_i + \beta_i, \ i = 2, \cdots, n \quad (11)$$

$$x_j - BoQ(t_j) = \epsilon_j, \ j \in B_p \quad (12)$$

$$x_j - BoQ(t_j) \geq -e_j, \ j \in V_p \quad (13)$$

$$x_j - BoQ(t_j) \leq e_j, \ j \in S_p \quad (14)$$

$$e_j \geq 0, \ \forall j \in V_p \cup S_p \quad (15)$$

$$0 \leq \alpha_i \leq w \quad (16)$$

Constraint Eq.(11) guarantees that the $(i-1)$th and the ith pieces of $BoQ(t)$ have the same value at π_i, so that the BoQ curve is continuous. Constraint Eq.(12) represents the fitting

errors of the BoQ curve on the critical points. Constraints Eq.(13)-Eq.(15) imply that the BoQ curve should separate the stopped trajectory points and the moving trajectory points. A penalty $e_j > 0$ is introduced if the trajectory point (t_j, x_j) cannot be classified into the correct state (i.e. moving or stopped). Constraint Eq.(16) is derived from the LWR kinematic wave theory, and guarantees that the slope of each piece of the BoQ curve is within the backward wave speed and 0. The objective function Eq.(10) aims to minimize the weighted error of fitting. The first term represents the total fitting error caused by the critical points; the second and the third term represent the total penalty caused by the failure to separate the moving and the stopped states; the fourth term attempts to control the number of linear segments in the BoQ to give a more robust solution. This is done by minimizing non-zero components in $\{\alpha_i - \alpha_{i-1}\}$, i.e. to make α_i and α_{i-1} as close as possible. Since the number of non-zero components in $\{\alpha_i - \alpha_{i-1}\}$ is not a convex function, an l_1 regularization term $\sum_{i=2}^{n} |\alpha_i - \alpha_{i-1}|$ is minimized instead as a convex approximation (1-norm approximation). By minimizing $\sum_{i=2}^{n} |\alpha_i - \alpha_{i-1}|$, the number of non-zero components in the set $\{\alpha_i - \alpha_{i-1}, \forall i\}$ can be approximately minimized. This technique is called $l1$-magic and often used in signal processing to reconstruct sparse signals (signals in which most components are zero). It is shown in [39] that this technique always yields a good approximation.

The regularization factors λ_1, λ_2 and λ_3 control how much weight should be given to each term of the objective function. Large λ_1 and λ_2 represent less tolerance on the misclassification of the moving and stopped states. Different weights λ_1 and λ_2 can also be given, if the importance of misclassification of the moving and stopped states are different. Large λ_3 will result in small number of breaks (i.e. segments) in the BoQ curve. These three parameters can be trained from the data by a cross-validation procedure.

Note that the formulation Eq.(10) - (16) is convex. Hence, the model can be solved easily with any convex optimization solver using the inner-point algorithm or Newton algorithm.

E. Calculation of the queue length

With the BoQ curve and FoQ curve of cycle p, the queuing region can be identified. The remaining queue from cycle p can be then calculated as the difference between them. Then, the queue length at time t is the summation of the remaining queues, i.e.

$$Q(t) = \sum_p \max\{FoQ_p(t) - BoQ_p(t), 0\} \quad (17)$$

III. REUSE OF UPSTREAM DEPARTURE INFORMATION FOR ARTERIAL-LEVEL ESTIMATION

In an urban arterial, if the intersections can communicate with each other, the departure information from the upstream intersection, calculated from the FoQ curve, can be beneficial for the queue estimation of the downstream intersection, especially in scenarios with low penetration rates. However, due to consideration of privacy and data transmission, it is not desirable to track the actual vehicle trajectories or share them

between intersections. In this section, we extend the general methodology proposed in Section II to integrate the estimated departure information from the upstream intersections to further improve the estimation accuracy at the arterial level while retaining vehicle privacy. This extended methodology follows two steps. In the first step, the arrival flow at the downstream intersection is estimated based on a platoon dispersion model (Section III-A); in the second step, such flow information is utilized for queue estimation (Section III-B).

A. Estimation of the arrival flow

Denote q_i as the flow that would have arrived at the intersection at time interval $\Pi_i = \{j | \pi_i \leq t_j < \pi_{i+1}\}$ in cycle p. We aim to estimate the flow q_i considering the information of the upstream intersection and the effect of platoon dispersion.

There are two cases based on whether the cycle $p-1$ at the downstream intersection is oversaturated.

In the first case, the flow q_i consists of the vehicles queued in cycle $p-1$, hence q_i is the saturation flow of the intersection.

In the second case, the flow q_i has not queued in the previous cycle. Instead, it comes from the upstream intersection. For an arterial, the discharging line at the upstream intersection provides prior arrival information to the downstream intersection. The departure flow from the upstream intersection can be zero (red time), the saturation flow (discharging), or the arrival flow at the intersection. However, due to the fluctuation of vehicle speeds, the discharging platoons from the upstream intersection tend to disperse over time and space. Hence, the vehicles discharged uniformly from the upstream signal would arrive at the downstream signal in a non-uniform manner, which makes the arrival flow at the downstream intersection different from the departure flow at the upstream intersection.

Many models depict the platoon dispersion [40]–[42]. However, the most widely used platoon dispersion model is Robertsons (1969). This model has become a virtual universal standard platoon dispersion model and has been implemented in various traffic simulation software, including TRANSYT [42], SCOOT [43] and TRAFLO [44]. In this paper, the Robertson's platoon dispersion model [42] is adopted to model the progression of vehicles between the two intersections. Note that other platoon dispersion models can also be incorporated in a similar way.

The Robertson's platoon dispersion model states that the downstream flow should be the linear combination of the previous downstream flow, and the corresponding upstream flow, i.e.

$$q_i = \frac{\rho T_f}{1 + \rho T_f} q_{i-1} + \frac{1}{1 + \rho T_f} q'_{i-T_f} \qquad (18)$$

where

- q_i is the arrival flow at the downstream intersection at time step i;
- q'_i is the departure flow from the upstream intersection at time step i;
- T_f is the free flow travel time between the two intersections with unit of time steps;

- ρ is a platoon dispersion factor expressing the degree of the dispersion of the platoon, which can be calibrated with empirical data [42].

The parameters T_f and ρ are constants if the configuration of the two intersections is given. The flow q'_{i-T_f} is given by the upstream intersection. The arriving flow at the downstream intersection can be calculated by Eq.(18).

B. Estimation of the queue length

Using the estimated arrival flow q_i and the kinematic wave theory, the slope of the BoQ curve at time interval Π_i can be calculated as

$$\hat{\alpha}_i = \frac{q_i}{q_i/u_f - k_{\text{jam}}} \qquad (19)$$

Then a regularization term can be added to Eq.(10) to integrate the information provided by the trajectory data and the flow data.

$$\min \frac{1}{2} \sum_{j \in B_p}^{n} \epsilon_j^2 + \lambda_1 \sum_{j \in S_p} e_j + \lambda_2 \sum_{j \in V_p} e_j + \lambda_3 \sum_{i=2}^{n} |\alpha_i - \alpha_{i-1}|$$
$$+ \gamma \sum_{i=1}^{n} \max\{\hat{\alpha}_i - \alpha_i, 0\} \qquad (20)$$

where γ is a weighting parameter balancing the trajectory data and the flow information. It represents our belief on the flow information. The more we trust the flow information and the more noisy the trajectory data is, the larger the γ should be. For low penetration rate and large noises in data, a large γ should be utilized. The regularization term aims to ensure that the $\hat{\alpha}_i \leq \alpha_i$. This is because the proposed methodology tends to underestimate the duration of the FoQ curve if the penetration rate is low and the last few vehicles in the queue are not connected. Therefore, the estimated slope $\hat{\alpha}_i$ is usually lower than the actual one α_i.

IV. INCLUSION OF THE INTERMEDIATE STATES FOR CASES WITH LIMITED DATA

This section extends the general methodology to explicitly handle the cases with low penetration rates and low sampling rates. One example of such cases is queue length estimation with probe taxi data or floating car data covering around 10% of the vehicles and reported every 10-30s. The potential problem in these cases is that there might not be enough trajectory points for the FoQ and BoQ estimation strictly following the methodology proposed in Section II. Recall that in order to estimate the FoQ or the BoQ curve in each cycle, we need at least one critical point. When the data is limited, however, there might not be a critical point for some cycles at all. This can be problematic, as the accurate estimation of both curves depends on the number of critical points we have. Thus, it is desirable to get as many critical points as possible. In this section, the data in the intermediate state (i.e. trajectory points with speed between $\underline{u}$ and $\bar{u}$) are used to provide information on acceleration and deceleration. With such information, more critical points can be estimated.

The estimation of critical points using the intermediate trajectory points follows two steps.

1) Identify the set of accelerating and decelerating trajectory points in each signal cycle p, respectively.

2) Estimate the critical points by fitting the acceleration and deceleration curves.

In the first step, denote A_p and D_p as the set of accelerating and decelerating trajectory points in signal cycle p, respectively. These trajectory points in A_p and D_p are determined by traversing each trajectory. Recall that in a normal cycle, the trajectory points are very likely to follow the order of states: accelerating, free flow state, decelerating, stopped state. Hence, considering two consecutive trajectory points in the same cycle where the earlier point j is an intermediate trajectory point ($j \in I_p$), and the later point j' is a free flow trajectory point ($j' \in V_p$) or an accelerating trajectory point ($j' \in A_p$) , we can deduce that the earlier trajectory point j is accelerating and assign it into A_p; Otherwise if an intermediate trajectory point $j \in I_p$ is right after a free flow trajectory point $j' \in V_p$ or a decelerating point $j' \in D_p$ in the same cycle, the trajectory point j should be decelerating and assigned into D_p. In the absence of free flow trajectory points (e.g. when the sampling rate is very low), it is more difficult to distinguish the accelerating and decelerating trajectory points. In such cases, we use the speed information. In cycle p, if the speed of a trajectory point is larger than the previous point along the same trajectory, we classify it as an accelerating trajectory point and assign it into set A_p. Otherwise we regard it as a decelerating trajectory point and assign it into set D_p.

It is assumed that all the vehicles have a uniform and constant acceleration rate a and deceleration rate d. Historical trajectory points can be used to calibrate both a and d. For a historical trajectory point j with speed v_j, denote Δx_j as the distance from the location of this trajectory point to the location where the vehicle stops (if available), then for each trajectory point j, it holds that

$$2a\Delta x_j = v_j^2 \text{ or } -2d\Delta x_j = v_j^2 \qquad (21)$$

Therefore, a and d can be estimated as

$$a = \frac{\sum_{j \in \bar{A}} v_j^2}{2 \sum_{j \in \bar{A}} \Delta x_j} \qquad (22)$$

$$d = -\frac{\sum_{j \in \bar{D}} v_j^2}{2 \sum_{j \in \bar{D}} \Delta x_j} \qquad (23)$$

where $\bar{A}$ and $\bar{D}$ denote the trajectory points in A and D if Δx_j is available, respectively. Note that even in scenarios with very low penetration rates and sampling rates, given a sufficiently long period of time, we can still obtain enough trajectory points for $\bar{A}$ and $\bar{D}$.

In the second step, we estimate the critical points using data points in A_p and D_p. The estimation of the critical points of the FoQ and BoQ curve with intermediate trajectory points are similar. In the rest of this section, for simplicity, we only present the estimation of the FoQ critical points. To adapt the following approach to the estimation of the BoQ curve, we only need to replace A_p and a with D_p and d, respectively.

With the constant acceleration assumption, the accelerating trajectory can be represented as a parabola.

$$x(t) = \frac{1}{2}at^2 + bt + c \qquad (24)$$

Then the estimation of the FoQ critical points follows two steps. In the first step, the accelerating trajectory Eq.(24) is estimated using the intermediate trajectory points in the set A_{p+1}. In the second step, the critical points are determined with the assistance of Eq.(24). For presentation simplicity, the two steps are described in details in Appendix A.

V. SIMULATION SETTINGS

This section describes the two datasets for evaluation: 1) the Lankershim dataset from the NGSIM project for undersaturated scenarios, and 2) the simulated data for oversaturated scenarios based on an arterial of Wehntalerstrasse, Zurich, Switzerland.

A. Under-saturated scenario: the Lankershim dataset from the NGSIM project

In the Lankershim dataset from the NGSIM project, all lanes with straight movements are considered (2 lanes). The study area is shown in Fig.3. The vehicle trajectory data correspond to the southbound trajectories from 8:30 a.m. to 8:45 a.m. (10 cycles) on June 16, 2005, see in Fig.4.
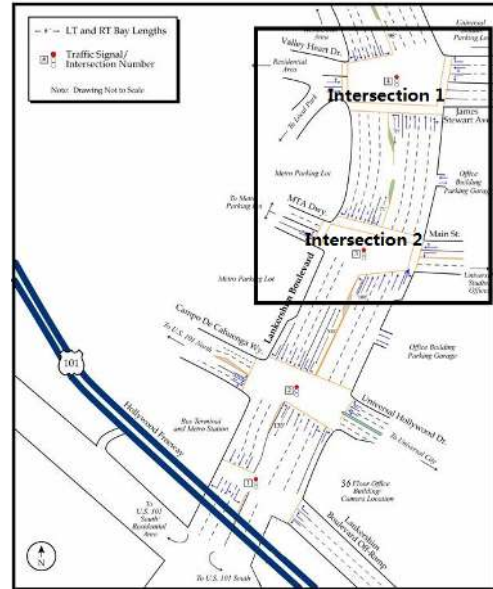

Fig. 3. The study area of the Lankershim dataset of NGSIM.

B. Over-saturated scenario: simulated dataset on Wehntalerstrasse, Switzerland

This dataset (thereafter called Wehntalerstrasse dataset) is based on the simulation of an arterial at Wehntalerstrasse, Zurich, Switzerland using VISSIM. We consider two intersections: 1) the intersection between Wehntalerstrasse and Einfangstrasse (Intersection 1, upstream), and 2) the intersection between Wehntalerstrasse and Glaubtenstrasse (Intersection 2,
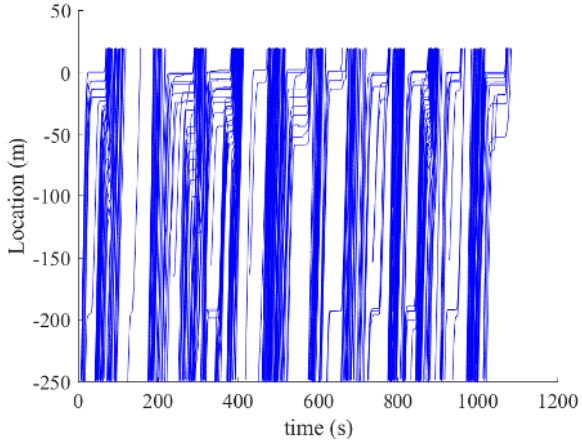
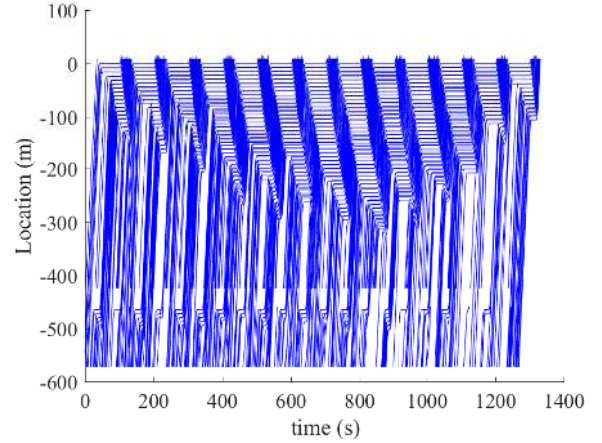Fig. 4. The vehicle trajectories in the Lankershim dataset.

Fig. 6. The vehicle trajectories in the Wehntalerstrasse dataset.

downstream). The considered arterial link has two lanes. The layout of the simulation is shown in Fig.5. This simulation model is calibrated and validated based on empirical measurements on Nov. 16, 2014. The simulated trajectory is illustrated in Fig.6 (13 cycles).

Fig. 5. The study area of the Wehntalerstrasse dataset.

C. Parameters for the simulation and evaluation criteria

TABLE II
PARAMETERS FOR SIMULATION

Parameter	Lankershim dataset	Wehntalerstrasse dataset
u_f [km/hr]	60	60
w [km/hr]	23.8	16.8
k_{jam} [veh/km]	200	250
T_f	17	40
γ	0.5	0.5
ρ	0.1	0.1
λ_1	1	1
λ_2	1	1
λ_3	0.5	0.5
$\underline{u}$ [m/s] 1	1	
$\bar{u}$ [m/s]	5	5
T_{step}[s]	2	2

The parameters for both scenarios are summarized in Table II. The performance of the proposed methodology is evaluated

by the mean estimation error, i.e. the average absolute difference between the estimated queue length and the actual queue length, i.e.

$$MAE = \frac{1}{t_f - t_0} \int_{t_0}^{t_f} |Q(t) - \hat{Q}(t)| \qquad (25)$$

where $\hat{Q}(t)$ is the estimated queue length at time t and $Q(t)$ is the ground truth queue length.

For the Lankershim dataset, the average queue length over time of the studied area is 3.0 cars, which means that if we estimate the queue length always as zero, we will get an MAE of 3.0 cars. For the Wehntalerstrasse dataset, the average queue length over time is 25.0 cars.

The model is solved using MATLAB with CVX toolbox [45], [46], a solver for convex optimization problems. The algorithm used by CVX tool box is the interior point method [47]. 10 random seeds are evaluated for each comparison.

VI. CASE STUDY AND RESULTS

This section shows the performance of the proposed method at both sites. Section VI-A shows the results for an isolated intersection. Section VI-B evaluates the benefit of considering a piecewise linear BoQ instead of a linear BoQ. Section VI-C demonstrates the benefit of considering the trajectory points in the intermediate state. The value of considering flow information is discussed in Section VI-D.

A. Results for an isolated intersection

In this section, the proposed methodology is evaluated at Intersection 2 in Fig.3 and Fig.5 for undersaturated case and oversaturated case, respectively. The resulting MAEs are shown in Fig.7. The penetration rate is set to vary between 0.05 and 1. The sampling rate is chosen to vary between $0.05\mathrm{s}^{-1}$ and $1\mathrm{s}^{-1}$. We found that the performance of the proposed methodology is not very sensitive to the sampling rate when the sampling rate is higher than $0.2\mathrm{s}^{-1}$. Therefore for illustration convenience, we only show the results with sampling rates $0.05\mathrm{s}^{-1}$ and $1\mathrm{s}^{-1}$. We can also see from
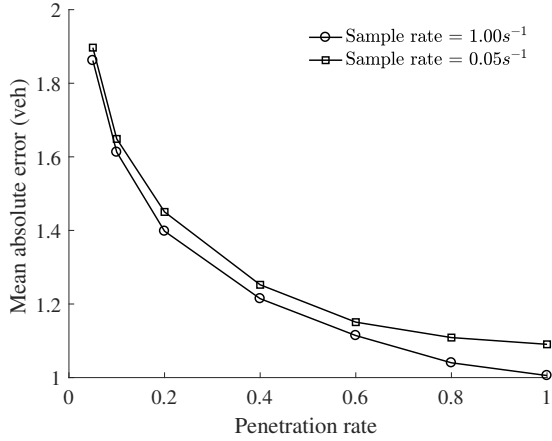
(a) Lankershim dataset
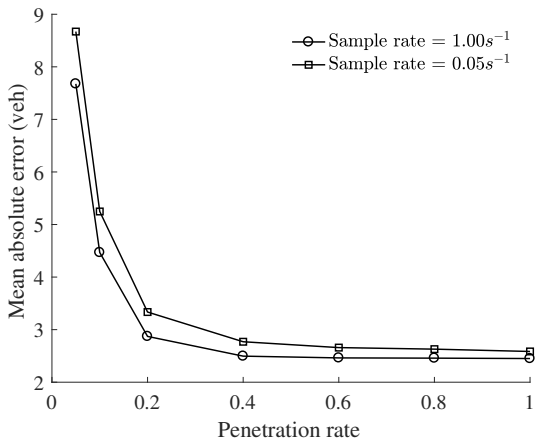
(b) Wehntalerstrasse dataset

Fig. 7. Performance of the proposed methodology for an isolated intersection.

Fig.7 that the proposed methodology is more sensitive to the penetration rate.

It can be seen from Fig.7a) and Fig.7b) that the estimation error decreases with the increase in penetration rate. The proposed methodology performs well for a relatively low penetration rate (0.1) and a low sampling rate (0.05s^{-1}), with the MAE less than 1.5 car for the Lankershim dataset and 5.2 cars for the Wehntalerstrasse dataset. This is expected, as for the undersaturated scenarios, the average queue length is small. Therefore, the error cannot be too large. For the oversaturated scenarios, however, as the absolute number of vehicles is large, having a penetration rate of 0.1 still gives sufficient critical points. However, the performance of the proposed methodology deteriorates as the penetration rate drops from 0.1 to 0.05, This is expected, because there are very few critical points, or even vehicle trajectories, in many cycles for such a low penetration rate. In such scenarios, it is hard to use deterministic methods to estimate the queue using only connected vehicle data. One solution could be stochastic models that can provide more robust results [20], [29]. We may also need other sources of information for queue length estimation in such scenarios.

The marginal benefit of having more connected vehicles decreases with the increase in the penetration rate. This suggests that the information provided by 40% can already yield satisfactory estimation results. We can also observe an error of on average 1 or 2 cars even for the 100% penetration rate and sampling rate of 1s^{-1}. This is because the driver behaviors in reality are stochastic and heterogeneous. The drivers do not exactly behave according to the traffic models. Note that here we assume the real penetration rate is not available to the proposed methodology. In addition, we perform the queue estimation for both lanes as a whole, which relies on the assumption that the queue length on both lanes are similar. However, the queue length may not be balanced on both lanes in reality. We may adapt the proposed methodology to lane-based queue estimation to improve the accuracy.

Comparing Fig.7a) and Fig.7b), we can see that the difference of the MAE between the two cases is small for moderate penetration rates (larger than 0.4). This is expected, as the estimation error of the queue length usually depends more on the last few vehicles in the queue, rather than the actual queue length. If the last few vehicles are all conventional vehicles, we tend to underestimate the queue length. Therefore, the estimation errors in the undersaturated scenarios and oversaturated scenarios are similar.

To get more detailed understanding of the proposed methodology, we demonstrates the time space diagram (Fig. 8a, Fig. 8c, Fig. 8e, and Fig. 8g) and the estimation of queue lengths (Fig. 8b, Fig. 8d, Fig. 8f, and Fig. 8h) of both sites with penetration rates (pr) of 0.2 and 1.0 for a particular random seed (42). In the time-space diagram, the green dashed lines represent all the trajectories that provide the ground truth, whereas the blue solid lines represent the trajectories of connected vehicles that we use for queue estimation. It can be seen from the time space diagrams (Fig. 8a, Fig. 8c, Fig. 8e, and Fig. 8g) that the proposed methodology is able to accurately estimate the FoQ and BoQ curve based on the information available. In scenarios with low penetration rates, the proposed methodology might fail to estimate the last few vehicles due to the lack of information. This can be verified from the queue length estimation (Fig. 8b, Fig. 8d, Fig. 8f, and Fig. 8h) where the proposed methodology tends to underestimate the queue length for scenarios with relatively low penetration rate. We can also see from Fig. 8b), Fig. 8d), Fig. 8f), and Fig. 8h) that even if the queue profiles are perfectly estimated, there could still be errors in the queue estimation due to the imbalance of the queue length on different lanes. Comparing Fig.8b) and Fig.8d) with Fig.8f) and Fig.8h), we can also see that the queue estimation process is more sensitive to low penetration rate in undersaturated scenarios than in oversaturated scenarios. This is The estimation error can be large, if very few vehicles arrive at the intersection, e.g. the fourth and sixth cycle in Fig.8a) and Fig.8b).

The cycle-by-cycle maximum queue length is shown in Table III and IV. It can be seen that the proposed proposed methodology can in general successfully estimate the FoQs, BoQs and queue lengths, even if the penetration rate is low.
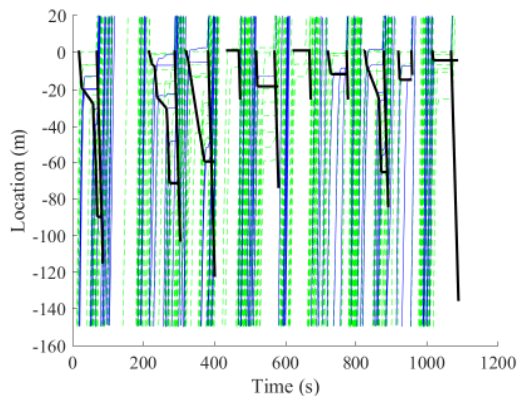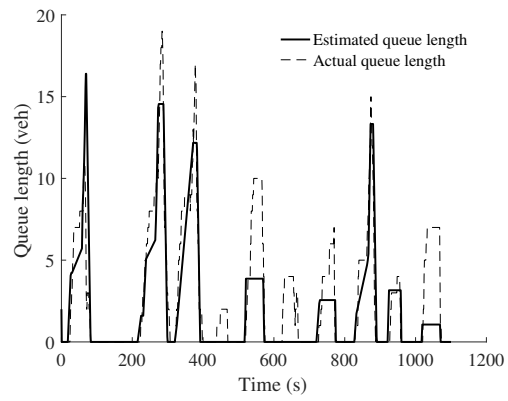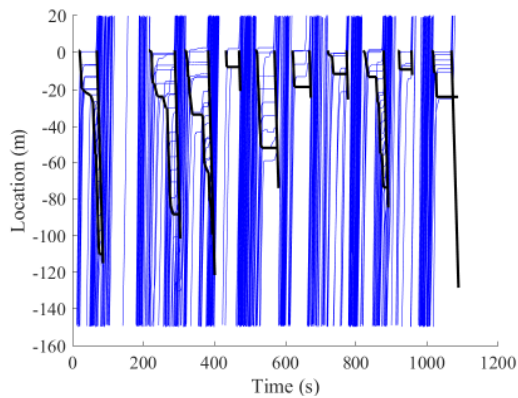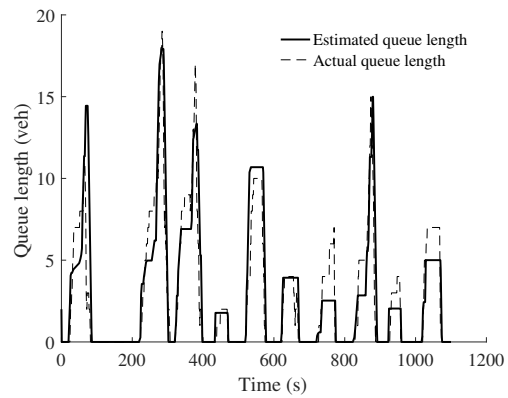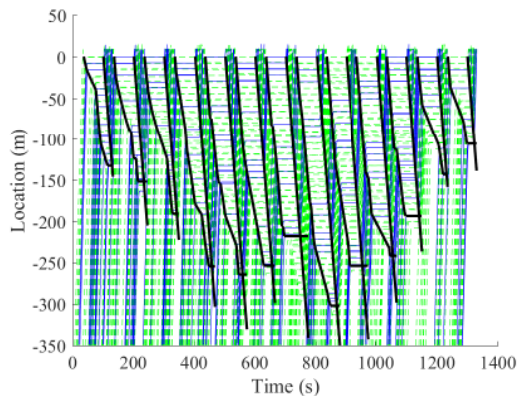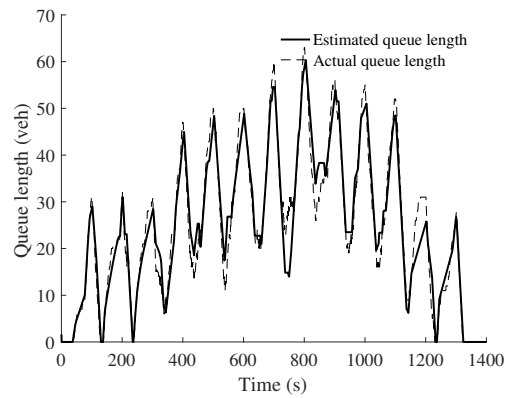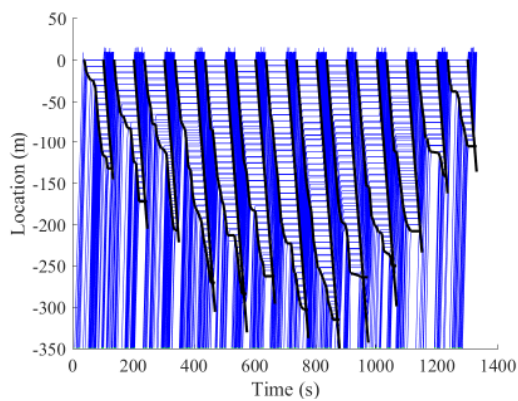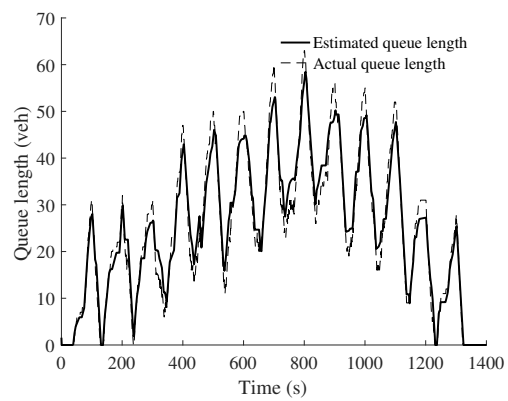
(a) Lankershim dataset, pr = 0.2, time space diagram

(b) Lankershim dataset, pr = 0.2, queue length

(c) Lankershim dataset, pr = 0.2, time space diagram

(d) Lankershim dataset, pr = 0.2, queue length

(e) Wehntalerstrasse dataset, pr = 1.0, time space diagram

(f) Wehntalerstrasse dataset, pr = 1.0, queue length

(g) Wehntalerstrasse dataset, pr = 1.0, time space diagram

(h) Wehntalerstrasse dataset, pr = 1.0, queue length

Fig. 8. Illustration of the time space diagrams and queue lengths. On the time space diagram, the green trajectories represent all the vehicle trajectories, whereas the blue trajectories represent the trajectory of connected vehicles. The bold black curves represent the FoQs and BoQs.

TABLE III
CYCLE-BY-CYCLE MAXIMUM QUEUE LENGTHS FOR LANKERSHIM
DATASET (SAMPLING RATE IS $1\mathrm{s}^{-1}$)

Cycle	Actual	pr = 0.2		pr = 1.0	
		Estimated	Error	Estimated	Error
1	11.0	11.9	0.9	11.4	0.4
2	19.0	14.6	4.4	17.9	1.1
3	17.0	12.2	4.8	13.1	3.9
4	2.0	0.0	2.0	1.8	0.2
5	10.0	3.9	6.1	10.7	0.7
6	4.0	0.0	4.0	3.9	0.1
7	7.0	2.6	4.4	2.5	4.5
8	15.0	13.3	1.7	15.0	0.0
9	4.0	3.2	0.8	2.0	2.0
10	7.0	1.1	5.9	5.0	2.0

TABLE IV
CYCLE-BY-CYCLE MAXIMUM QUEUE LENGTHS FOR
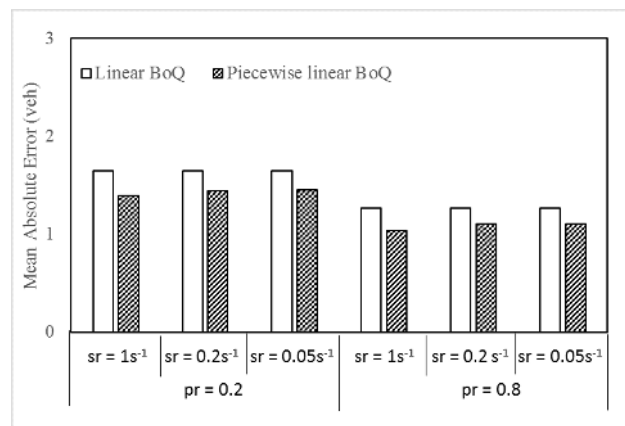WEHNTALERSTRASSE DATASET (SAMPLING RATE IS $1\mathrm{s}^{-1}$)

Cycle	Actual	pr = 0.2		pr = 1.0	
		Estimated	Error	Estimated	Error
1	31.0	28.6	2.4	28.9	2.1
2	30.0	29.9	0.1	29.9	0.1
3	30.0	27.9	2.1	27.5	2.5
4	47.0	42.8	4.2	43.4	3.6
5	50.0	46.6	3.4	46.1	3.9
6	50.0	47.9	2.1	46.0	4.0
7	60.0	54.6	5.4	54.4	5.6
8	63.0	58.6	4.4	58.7	4.3
9	56.0	52.6	3.4	51.1	4.9
10	55.0	50.1	4.9	50.6	4.4
11	52.0	48.5	3.5	49.0	3.0
12	31.0	25.3	5.7	28.4	2.6
13	27.0	26.4	0.6	25.9	1.1

(a) Lankershim dataset

(b) Wehntalerstrasse dataset

Fig. 9. Value of considering piecewise linear BoQ.

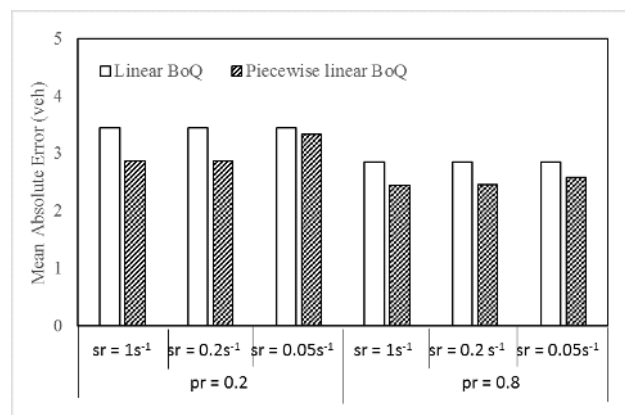## B. Value of considering piecewise linear BoQ

In order to evaluate the benefit of considering the piecewise linear BoQ curve, we compare the results with a state-of-art method [26] that assumes constant demand within a cycle, and thus a linear BoQ between the maximum queue length and the minimum queue length[1]. However, note that the demand in both datasets is not constant within a signal cycle, because it is affected by the traffic signal in the downstream intersection. In scenarios with a more uniform demand within the signal cycle, the two methods yield similar results. We test the scenarios with penetration rates (pr) of 0.2 and 0.8, and sampling rate (sr) of $1\mathrm{s}^{-1}$, $0.2\mathrm{s}^{-1}$ and $0.05\mathrm{s}^{-1}$. The results are shown in Fig.9. The results for the proposed algorithm and the algorithm in [26] are shown in the blank bar and the shaded bar, respectively. Note that the algorithm in [26] is based on sample travel times, assuming that the arrival times on two virtual lines are available. Therefore, the results for different sampling rates are the same.

It can be seen that considering a piecewise linear BoQ can improve the accuracy in estimation (up to 0.6 car and 16%). This shows that we can reduce the systematic errors caused by non-uniform arrivals. It is also shown that the improvement is in general larger for scenarios with higher sampling rates and higher penetration rates. This is because in such scenarios, the

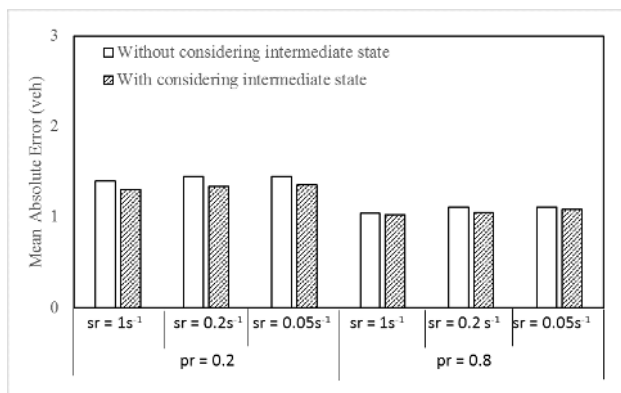BoQ is more likely to be non-linear.

C. Value of considering acceleration and deceleration

The value of considering the intermediate state is shown in Fig.10. The shaded bars represent the estimation results of the extended methodology considering intermediate state proposed in Section IV, and the white bars represent the estimation results of the general methodology without including acceleration and deceleration information.
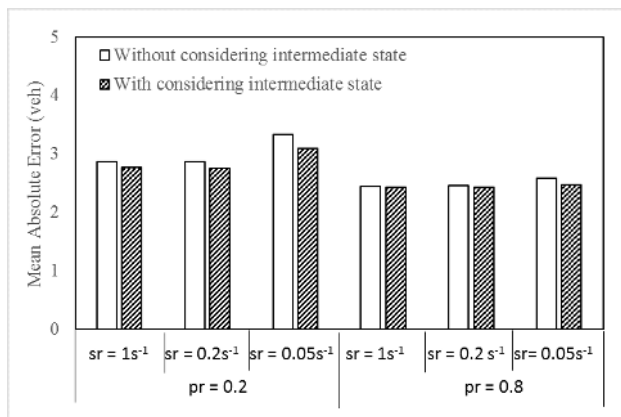
We can conclude that the method proposed in Section IV successfully reduces the estimation error in all scenarios tested. The improvement is up to 0.1 car and 6%. Generally speaking, the benefit of this method is larger in scenarios with low penetration rates and/or low sampling rates. In such scenarios, the reported trajectory points are very few. Hence, to get sufficient critical points, the intermediate state should be taken into account. However, in scenarios with high penetration rates and/or high sampling rates, e.g. $pr = 0.8$ and $sr = 1\mathrm{s}^{-1}$, the benefit of considering the intermediate state is marginal. Therefore, it is advised to consider the intermediate state only if either the sampling rate or the penetration rate is low.

D. Value of integrating flow information

This section evaluates the value of integrating the upstream departure information at the arterial level by comparing the

---

[1]In undersaturated scenarios, the method in [26] estimates a linear BoQ, as the minimum queue length is 0. While in oversaturated scenarios, the resulting BoQ from [26] can have two linear segments.

(a) Lankershim dataset

(b) Wehntalerstrasse dataset

Fig. 10. Value of considering acceleration and deceleration.

(a) Lankershim dataset

(b) Wehntalerstrasse dataset
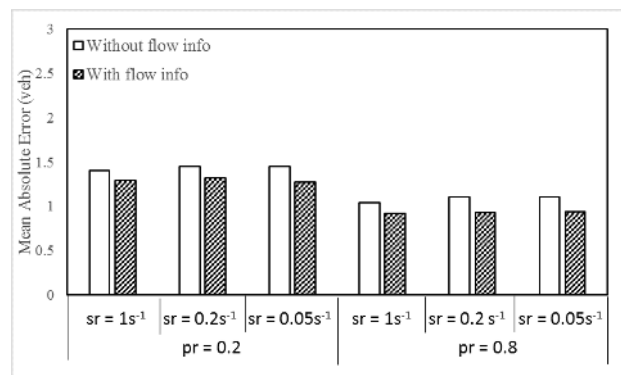
Fig. 11. Value of flow information.

extended methodology for the arterial level (Section III) to the general methodology. The departure flow from Intersection 1 at both sites is integrated with a Robertson's platoon dispersion model. The results are shown in Fig.11.
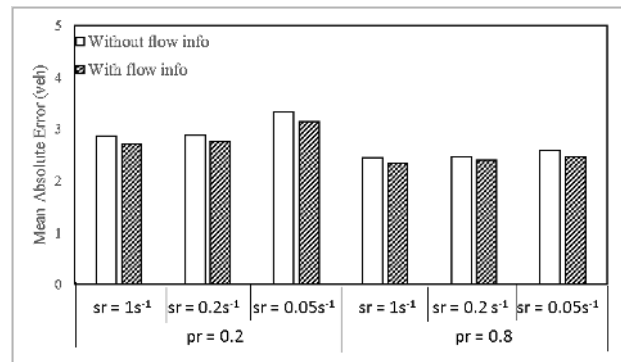
Fig.11 shows that the flow information from the upstream intersection improves the performance of the algorithm in all scenarios tested. The improvement is up to 0.2 car and 16%. It can also be seen that trend is similar in both types of scenarios. However, the algorithm benefits more from the flow information in the undersaturated scenarios. This is because in undersaturated scenarios, there are not many trajectories. Therefore, additional information given by the upstream intersection is more valuable.

VII. SENSITIVITY ANALYSIS OF THE PROPOSED METHODOLOGY

In this section, we analyze various aspect of the proposed methodology. First, the sensitivity to the model parameters is analyzed in Section VII-A. Second, the robustness of the proposed algorithm is evaluated in Section VII-B. Finally, the computation time of the proposed algorithm is tested in Section VIII-B. For presentation simplicity, the results of this section are only based on the Lakershim dataset (Section V-A). The results of the Wehntalerstrasse dataset (Section V-B) exhibit similar properties.

A. Sensitivity analysis to model parameters

This section discusses the sensitivity of the proposed methodology to the model parameters: the regularization term λ_1, λ_2 and λ_3, the time step T_{step} for the BoQ estimation, the lower speed bound $\underline{u}$, the upper speed bound $\bar{u}$, and the parameters for the fundamental diagram w, u_f and k_{jam}. The aim is to evaluate the impact of each parameter on the performance of the proposed methodology if it deviates from the optimal values. To do this, we use a One-at-a-time sensitivity analysis method. Specifically, we change one parameter at each time and fix the other parameters at their optimal value, and observe how this influences the performance. In this way, we obtain the local sensitivity to this parameter. Note that this local sensitivity analysis is already enough for practical applications, because we do not expect the parameter values to deviate a lot from the optimal values.

In the rest of this subsection, λ_1, λ_2 and λ_3 are chosen to vary between 0.5 and 2, T_{step} between 1s and 10s, the lower speed bound $\underline{u}$ between 1m/s and 6m/s, the upper speed bound $\bar{u}$ between 6m/s and 10m/s, u_f between 50km/h and 70km/h, w between 15km/hr and 25km/hr, and k_{jam} between 160veh/km and 240veh/km.

The results show that the proposed methodology is not sensitive to the regularization factors λ_1, λ_2 and λ_3, the upper and lower speed bounds $\underline{u}$ and $\bar{u}$, the free flow speed u_f and the backward wave speed w. This is expected, as the regularization factors λ_1 and λ_2 penalize the FoQ and BoQ curves if they misclassify the stopped state and free-
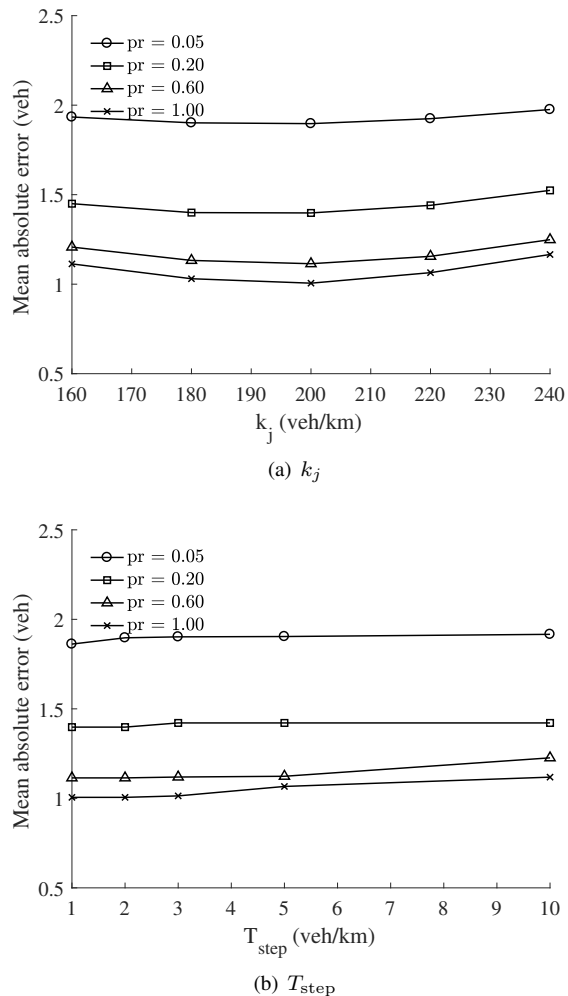
(a) k_j

(b) T_{step}

Fig. 12. Sensitivity analysis to model parameters. Sampling rate = 1.0s^{-1}.

flow states; λ_3 controls the number of pieces in the piecewise linear BoQ curve. In reality, as there are not many trajectory points, the probability of misclassification and the number of pieces in the piecewise linear BoQ curve are both quite small. The free flow speed u_f and the backward wave speed w can be fitted from the trajectory points, therefore their specific values are not important for the model. For the upper and lower speed bounds $\underline{u}$ and $\bar{u}$, the probability of the trajectory points falling into the speed range of [1m/s, 3m/s] and [8m/s, 10m/s] is small if the links are not oversaturated. Therefore the proposed method is not sensitive to the specific values of the speed bounds. However, in scenarios with over-saturated links where the vehicles frequently accelerate and decelerate, these two parameters might be important.

Fig.12 shows the sensitivity analysis for the sensitive parameters, k_{jam} and T_{step}. As is shown in Fig. 12a), the model is sensitive to the jam density k_{jam}. This is reasonable, as the jam density is used to calculate the queue length from the BoQ and FoQ curves. Inaccurate jam density will lead to inaccurate queue length estimation, even if the BoQ and FoQ curves are accurate. It is shown in Fig. 12b) that the proposed methodology is also sensitive to T_{step}. If T_{step} is

too large, there would be a large discretization error in the BoQ curve. Hence, the queue estimation error increases. It is also observed that the proposed methodology performs similar for a T_{step} of 1s to 3s. This is because these values of T_{step} are already smaller than the vehicle headway. So the marginal benefit of further reducing T_{step} is negligible. This suggests that the value of T_{step} should be chosen as 1-3s, and the value of k_{jam} should be as accurate as possible (e.g. obtained from the real data).

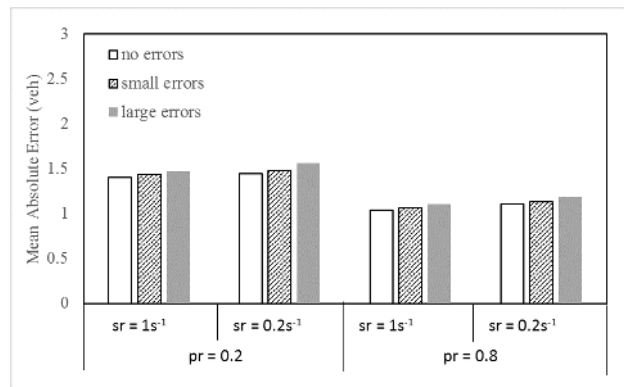### B. Robustness to measurement errors

Fig. 13. Sensitivity to the measurement errors, where small error represents a standard error of 2m for location and 0.5m/s for speed, and large error represents a standard error of 10m for location and 2m/s for speed.

Due to the errors in the measurement devices, the location and speed information received by the central controller may be inaccurate. This section tests how the errors in location affects the performance of the proposed methodology. It is assumed that both the location and speed errors follow a Gaussian distribution with mean 0, which means that there are no systematic errors. The standard deviation of the location measurement is assumed to vary between 0 and 10m. This is because the normal GPS devices provide an accuracy of 7.8 meters at 95% confidence level [48], and the accuracy can also be enhanced by map-matching [49], Kalman filter [6], or data fusion with other in-vehicle sensors [50]. The variance of the speed errors is assumed to be between 0 and 2m/s. The location errors and the speed errors are assumed to be independent. The errors at different time steps are also assumed to be independent.

The effects of the measurement errors are shown in Fig.13. It can be seen that the mean absolute error increases only slightly with the standard deviation of the measurement error (up to 2% for small errors and 7% for large errors). Therefore, the proposed model is robust to measurement errors.

VIII. IMPLEMENTATION DETAILS

A. Online Implementation

In this section, we present the online implementation details of the proposed methodology for real-time queue estimation. For simplicity of the presentation, we only describe the details for the general methodology in Section II. The extensions in Section III-IV can be treated in a similar way.

At time t, we define a cycle p as an "active cycle", if the queue due to the red signal in cycle p is still active at time t, i.e. the remaining queue of cycle p is positive ($FOQ_p(t) - BOQ_p(t) > 0$). Note that there could be more than one active cycles at each time t, as the proposed methodology can be used for both undersaturated and oversaturated scenarios. Then, estimating the queue length at time t can be formulated as calculating the FoQ and BoQ curves of all active cycles, using the available trajectory information up to time t. Let us denote the set of all the active cycles at time t as P_t. The general implementation framework is summarized into Algorithm 1, as follows.

Algorithm 1 General Online Implementation Framework of the Algorithm

---

Initialize: $P_0 = \emptyset$,
1:   **for** $t = T_e,\ 2T_e,\ \cdots$ **do**
2:       **if** $t - T_e < r_p \le t$ **then**
3:          $P_t = P_{t-T_e} \cup \{p\}$
4:       **for** $p \in P$ **do**
5:          Update S_p, V_p, F_p and B_p with newly received trajectory points, and obtain FOQ_p and BOQ_p
6:          **if** $FOQ_p(t - T_e) - BOQ_p(t - T_e) > 0$ and $FOQ_p(t) - BOQ_p(t) \le 0$ **then**
7:             $P_{t+T_e} = P_t \backslash \{p\}$
8:       Calculate queue length $Q(t)$ using Eq.(17)

In Algorithm 1, T_e represents the time step to perform queue estimation. At each time t, the algorithm first check if there is a new cycle (lines 2-3) and update the set of active cycles P accordingly. Line 5 represents the general methodology, for which there are two ways to implement. The first approach, hereafter named direct implementation approach, applies the exact procedure described in Section II. We update the sets of trajectory points S_p and V_p based on Section II-A, calculate the critical points based on Section II-B, and obtain the FoQ curve and BoQ curve by solving Eq.(4)-(8) (Section II-C) and Eq.(10)-(16) (Section II-D), respectively. It will be shown in Section VIII-B that this implementation approach is sufficiently efficient for most real-time traffic control (e.g. signal control) algorithms.

The second approach, hereafter named simplified implementation approach, further reduces the computation time and the memory requirement. Specifically, we have three simplifications. First, instead of the entire set of trajectory points, we only store the mean and total number of the trajectory points of vehicle m in state s (stopped or free flow) in each cycle p, denoted as $(\bar{t}^s_{m,p}, \bar{x}^s_{m,p})$ and $n^s_{m,p}$, respectively. These values are updated every time when new trajectory information is received. Then, the FoQ and BoQ critical points are calculated in a similar way as in Section II-B where $J_m \cap S_p$ is replaced by the stopped mean trajectory point and $J_m \cap V_p$ is replaced by the free flow trajectory points. Second, when calculating the set of stopped (or free flow) trajectory points S_p (or V_p), we only keep the first and the last stopped (or free flow) trajectory points of each vehicle in cycle p, which can be seen as the supporting vectors for constraints Eq.(6) and Eq.(14) (or Eq.(7) and (13)). Third, we only keep the critical points, stopped and trajectory points with a time stamp shortly before t (i.e. in

range $(t - \delta t, t]$). This is because the BoQ and FoQ curves are influenced mainly by the information around time t.

After the FoQ and BoQ curve for cycle p is obtained, we check if the cycle p is still active (i.e. queue of cycle p is fully discharged) by comparing the obtained FOQ and BOQ curve. If cycle p is no longer active, we remove cycle p from the set of active cycles. This procedure is illustrated in lines 6-7 in Algorithm 1. After FOQ and BOQ curves are calculated for all the active cycles, the queue length is calculated using Eq.17 (line 8).

B. Comparison between the two implementation approaches

The two online implementation approaches are tested on the Intersection 2 of Lankershim and Wehntalerstrasse datasets. From the description of the general framework and two online implementation approaches, the simplified approach requires significantly less memory than the direct approach, as only a small fraction of trajectory points need to be stored. In this subsection, we evaluate the average time and the mean absolute error of both approaches. The results are summarized in Fig. 14. Fig. 14a) shows the average computation time in one time step, and Fig. 14b) shows the mean absolute error of the online solution of both approaches compared to the ground truth. Here, δt is chosen as 10s.

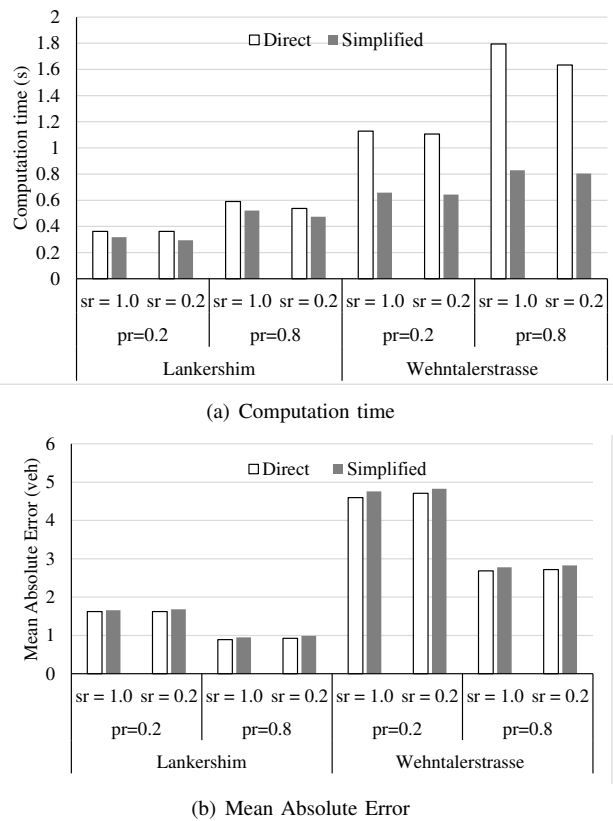(a) Computation time

(b) Mean Absolute Error

Fig. 14. Comparison between two online implementation approaches: the direct approach and the simplified approach.

It can be seen from Fig.14 that the direct approach can yield satisfactory results within 2s and the simplified approach takes less than 0.8s. This shows that both approaches are

sufficiently efficient for most applications (e.g. signal control). The simplified approach performs similarly to the direct approach in terms of the estimation accuracy (only up to 5% worse). However, the simplified approach significantly reduces the computation time. The improvement is up to 18% for Lankershim dataset and 54% for Wehntalerstrasse. This shows that the simplified approach performs especially well for oversaturated scenarios. Another observation is that the computation time increases as the penetration rate and the sampling rate increase. This is expected, as the amount of information increases, thus the optimization model has more variables. Our experiments also show that the results are not sensitive to the size of the discretization time step, thus we can choose a smaller discretization time for a better accuracy.

IX. CONCLUSION

This paper proposes a methodology to estimate the queue length in a connected vehicle environment. A convex model is formulated to calculate a linear FoQ curve and a piecewise linear BoQ curve. The queue length can be represented as the difference between the two curves. This paper further proposes a framework to perform arterial level estimation, reusing the estimated discharging rate of the upstream intersection . The cases with low sampling rate are also handled by utilizing the trajectory data in the intermediate state.

A validation experiment with the Lankershim dataset and Wehntalerstrasse dataset shows that the convex model performs well. The average estimation error is within 1.5 cars for undersaturated scenarios and 5.2 cars for oversaturated scenarios, with penetration rates larger than 0.1 and sampling rates higher than 0.05s^{-1}. Compared to a state-of-art method that assumes linear BoQ, the proposed algorithm improves the estimation accuracy by up to 16%. For an arterial, the performance of the proposed methodology is further enhanced by the departure flow information at the upstream intersection, with an improvement of up to 16%. It is also shown that the proposed methodology works well under the low sampling rate, and is relatively robust to measurement errors.

This paper relies on the assumption of a fundamental diagram and a few parameters. It is shown that the proposed methodology is only sensitive to the assumed jam density and the time step for back of queue estimation T_{step}. It is expected that the performance of the proposed methodology is not sensitive to the shape of the fundamental diagram, as long as the jam density is well calibrated.

We further propose two online implementation approaches for real-time queue estimation. Results show that the direct approach that uses the exact offline algorithm takes less than 2s for one estimation step, and an simplified approach takes less than 0.8s for each estimation step. This shows that the convexity of the method ensures the efficiency in computation, which is sufficient for most applications.

The output of the proposed methodology is the queue profile, which can be used in trajectory reconstruction, delay evaluation, flow and density estimation, etc. The proposed methodology can be beneficial to designing and evaluating signal control algorithms, which is considered as the future work of the authors.

APPENDIX A
INCLUSION OF THE INTERMEDIATE STATES FOR CASES WITH LIMITED DATA (CONTINUED)

This appendix elaborates the procedure for estimating the FoQ critical points when the sampling rates are low. Particularly, we consider three cases:

1) There are stopped trajectory points but no free flow trajectory points, i.e. set $V_{p+1} \cap J_m = \emptyset$ and set $S_p \cap J_m \neq \emptyset$;
2) There are free flow trajectory points but no stopped trajectory points, i.e. set $V_{p+1} \cap J_m \neq \emptyset$ and set $S_p \cap J_m = \emptyset$;
3) There are neither free flow trajectory points nor stopped trajectory points, i.e. set $V_{p+1} \cap J_m = \emptyset$ and set $S_p \cap J_m = \emptyset$.

For case 1) and 2), we assume that there is at least one trajectory point in the set A_{p+1}. For case 3), we assume that there are at least two trajectory points in $A_{p+1} \cap J_m$ for at least one vehicle trajectory m. This is the least requirement to guarantee that we can reconstruct at least one critical point.

The procedure has two steps. In the first step, we estimate the accelerating trajectory, i.e. the value of b and c in Eq.(24). In the second step, the critical points are obtained based on the accelerating trajectory. In the rest of this section, we explain the procedure for the three cases, respectively.

For case 1), we denote the line fitted from the stopped trajectory points in set $J_m \cap S_p$ as $x(t) = l_m^p$. This line has a slope of zero, as it represents the stopped state. Then the following two properties should hold. First, Eq.(24) should be tangent to line $x(t) = l_m^p$. This is because both the location and the speed are continuous. Second, the distance between Eq.(24) and the trajectory points in set $J_m \cap A_{p+1}$ should be minimized.

Based on these two properties, we can build an optimization model for trajectory m.

$$\min \sum_{j \in J_m \cap A_{p+1}} (\frac{1}{2}at_j^2 + bt_j + c - x_j)^2 \qquad (26)$$

$$\text{s.t. } 2ac - b^2 = 2al_m^p \qquad (27)$$

where the constraints and the objective function correspond to the two properties, respectively. The decision variables are b and c. Although Eq.(26) and Eq.(27) are not convex, the optimal solution of b and c can be represented in a closed form. Therefore, it is not necessary to solve the model Eq.(26) and Eq.(27) in practice.

With the estimated trajectory in the intermediate state, we can reconstruct the trajectory in the free flow state as a tangent line to the parabola Eq.(24) with slope u_f. With a basic calculation, the critical point can be represented as $\left(\dfrac{u_f - 2b}{2a}, l_m^p \right)$.

For Case 2), let us denote the trajectory fitted from the free-flow trajectory points in set $J_m \cap V_{p+1}$ as the line $x = u_m^p t + \eta_m^p$. Similarly to Case 1) in Section IV, the parabola Eq.(24) should also satisfy the following two requirements.

1) Eq.(24) should be tangent to line $x = u_m^p t + \eta_m^p$. This is because both the location and the speed are continuous.

2) The distance between Eq.(24) and the trajectory points in set $J_m \cap A_{p+1}$ should be minimized.

Then we formulate the following optimization model

$$\min \sum_{j \in J_m \cap A_{p+1}} \left(\frac{1}{2}at_j^2 + (b + u_m^p)t_j + c - x_j\right)^2 \quad (28)$$

$$\text{s.t. } 2ac - b^2 = 2a\eta_m^p \quad (29)$$

Model Eq.(28) and Eq.(29) can also be transformed into a cubic equation and solved analytically. Then the critical point can be represented as $\left(\dfrac{u_f - 2b}{2a}, c - \dfrac{b^2}{2a}\right)$.

For Case 3), as there are no trajectory points in either the free flow state or the stopped state, we only require that the distance between Eq.(24) and the trajectory points in set $J_m \cap A_{p+1}$ be minimized. Hence we have the following non-constrained optimization problem.

$$\min \sum_{j \in J_m \cap A_{p+1}} \left(\frac{1}{2}at_j^2 + bt_j + c - x_j\right)^2 \quad (30)$$

Model Eq.(30) is a convex model, which can be transformed into a set of linear equations. Then the critical point can be represented as $\left(\dfrac{u_f - 2b}{2a}, c - \dfrac{b^2}{2a}\right)$.

REFERENCES

[1] F. Webster, "Traffic signal settings, road research laboratory techn. rep. no. 39," 1958.

[2] R. E. Allsop, "Delay-minimizing settings for fixed-time traffic signals at a single road junction," *IMA Journal of Applied Mathematics*, vol. 8, no. 2, pp. 164–185, 1971.

[3] T.-H. Chang and J.-T. Lin, "Optimal signal timing for an oversaturated intersection," *Transportation Research Part B: Methodological*, vol. 34, no. 6, pp. 471 – 491, 2000. [Online]. Available: http://www.sciencedirect.com/science/article/pii/S019126159900034X

[4] S. I. Guler, M. Menendez, and L. Meier, "Using connected vehicle technology to improve the efficiency of intersections," *Transportation Research Part C: Emerging Technologies*, vol. 46, pp. 121–131, 2014.

[5] L. Li, K. Yang, Z. Li, and Z. Zhang, "The optimality condition of the multiple-cycle smoothed curve signal timing model," *Transportation Research Part C: Emerging Technologies*, vol. 27, pp. 46 – 57, 2013, selected papers from the Seventh Triennial Symposium on Transportation Analysis (TRISTAN VII). [Online]. Available: http://www.sciencedirect.com/science/article/pii/S0968090X12001507

[6] K. Yang, S. I. Guler, and M. Menendez, "Isolated intersection control for various levels of vehicle technology: Conventional, connected, and automated vehicles," *Transportation Research Part C: Emerging Technologies*, vol. 72, pp. 109–129, 2016.

[7] K. Yang, N. Zheng, and M. Menendez, "Multi-scale perimeter control approach in a connected-vehicle environment," *Transportation Research Part C: Emerging Technologies*, 2017.

[8] K. Yang, M. Menendez, and S. I. Guler, "Implementing transit signal priority in a connected vehicle environment with and without bus stops," *Transportmetrica B: Transport Dynamics*, pp. 1–23, 2018.

[9] K. N. Balke, H. A. Charara, and R. Parker, "Development of a traffic signal performance measurement system (tspms)," Texas Transportation Institute, Texas A & M University System, Tech. Rep., 2005.

[10] A. Skabardonis and N. Geroliminis, "Real-time monitoring and control on signalized arterials," *Journal of Intelligent Transportation Systems*, vol. 12, no. 2, pp. 64–74, 2008.

[11] X. Zhan, R. Li, and S. V. Ukkusuri, "Lane-based real-time queue length estimation using license plate recognition data," *Transportation Research Part C: Emerging Technologies*, vol. 57, pp. 85 – 102, 2015.

[12] H. X. Liu, X. Wu, W. Ma, and H. Hu, "Real-time queue length estimation for congested signalized intersections," *Transportation Research Part C: Emerging Technologies*, vol. 17, no. 4, pp. 412 – 427, 2009.

[13] J. C. Herrera, D. B. Work, R. Herring, X. J. Ban, Q. Jacobson, and A. M. Bayen, "Evaluation of traffic data obtained via gps-enabled mobile phones: The mobile century field experiment," *Transportation Research Part C: Emerging Technologies*, vol. 18, no. 4, pp. 568–583, 2010.

[14] L. Ambühl and M. Menendez, "Data fusion algorithm for macroscopic fundamental diagram estimation," *Transportation Research Part C: Emerging Technologies*, vol. 71, pp. 184–197, 2016.

[15] Z. Sun and X. J. Ban, "Vehicle trajectory reconstruction for signalized intersections using mobile traffic sensors," *Transportation Research Part C: Emerging Technologies*, vol. 36, pp. 268–283, 2013.

[16] P. Gómez, M. Menéndez, and E. Mérida-Casermeiro, "Evaluation of trade-offs between two data sources for the accurate estimation of origin–destination matrices," *Transportmetrica B: Transport Dynamics*, vol. 3, no. 3, pp. 222–245, 2015.

[17] I. Dakic and M. Menendez, "On the use of lagrangian observations from public transport and probe vehicles to estimate car space-mean speeds in bi-modal urban networks," *Transportation Research Part C: Emerging Technologies*, vol. 91, pp. 317–334, 2018.

[18] G. Comert and M. Cetin, "Queue length estimation from probe vehicle location and the impacts of sample size," *European Journal of Operational Research*, vol. 197, no. 1, pp. 196 – 202, 2009.

[19] G. Comert, "Simple analytical models for estimating the queue lengths from probe vehicles at traffic signals," *Transportation Research Part B: Methodological*, vol. 55, pp. 59–74, 2013.

[20] ——, "Effect of stop line detection in queue length estimation at traffic signals from probe vehicles data," *European Journal of Operational Research*, vol. 226, no. 1, pp. 67–76, 2013.

[21] Z. Amini, R. Pedarsani, A. Skabardonis, and P. Varaiya, "Queue-length estimation using real-time traffic data," in *Intelligent Transportation Systems (ITSC), 2016 IEEE 19th International Conference on*. IEEE, 2016, pp. 1476–1481.

[22] M. J. Lighthill and G. B. Whitham, "On kinematic waves. ii. a theory of traffic flow on long crowded roads," in *Proceedings of the Royal Society of London A: Mathematical, Physical and Engineering Sciences*, vol. 229. The Royal Society, 1955, pp. 317–345.

[23] M. Lighthill and G. Whitham, "On kinematic waves. i. flood movement in long rivers," in *Proceedings of the Royal Society of London A: Mathematical, Physical and Engineering Sciences*, vol. 229. The Royal Society, 1955, pp. 281–316.

[24] P. I. Richards, "Shock waves on the highway," *Operations research*, vol. 4, no. 1, pp. 42–51, 1956.

[25] X. Ban, R. Herring, P. Hao, and A. Bayen, "Delay pattern estimation for signalized intersections using sampled travel times," *Transportation Research Record: Journal of the Transportation Research Board*, no. 2130, pp. 109–119, 2009.

[26] X. J. Ban, P. Hao, and Z. Sun, "Real time queue length estimation for signalized intersections using travel times from mobile sensors," *Transportation Research Part C: Emerging Technologies*, vol. 19, no. 6, pp. 1133 – 1156, 2011.

[27] P. Hao, X. Ban, K. P. Bennett, Q. Ji, and Z. Sun, "Signal timing estimation using sample intersection travel times," *IEEE Transactions on Intelligent Transportation Systems*, vol. 13, no. 2, pp. 792–804, 2012.

[28] P. Hao, X. J. Ban, D. Guo, and Q. Ji, "Cycle-by-cycle intersection queue length distribution estimation using sample travel times," *Transportation research part B: methodological*, vol. 68, pp. 185–204, 2014.

[29] P. Hao and X. Ban, "Long queue estimation for signalized intersections using mobile data," *Transportation Research Part B: Methodological*, vol. 82, pp. 54–73, 2015.

[30] P. Izadpanah, B. Hellinga, and L. Fu, "Automatic traffic shockwave identification using vehicles trajectories," in *Proceedings of the 88th Annual Meeting of the Transportation Research Board (CD-ROM)*, 2009.

[31] G. Hiribarren and J. C. Herrera, "Real time traffic states estimation on arterials based on trajectory data," *Transportation Research Part B: Methodological*, vol. 69, pp. 19 – 30, 2014.

[32] Y. Cheng, X. Qin, J. Jin, and B. Ran, "An exploratory shockwave approach to estimating queue length using probe trajectories," *Journal of Intelligent Transportation Systems*, vol. 16, no. 1, pp. 12–23, 2012.

[33] M. Ramezani and N. Geroliminis, "Queue profile estimation in congested urban networks with probe data," *Computer-Aided Civil and Infrastructure Engineering*, vol. 30, no. 6, pp. 414–432, 2015. [Online]. Available: http://dx.doi.org/10.1111/mice.12095

[34] B. Mehran, M. Kuwahara, and F. Naznin, "Implementing kinematic wave theory to reconstruct vehicle trajectories from fixed and probe sensor data," *Transportation research part C: emerging technologies*, vol. 20, no. 1, pp. 144–163, 2012.

[35] V. Alexiadis, J. Colyar, J. Halkias, R. Hranac, and G. McHale, "The next generation simulation program," *Institute of Transportation Engineers. ITE Journal*, vol. 74, no. 8, p. 22, 2004.

[36] N. Chiabaut, C. Buisson, and L. Leclercq, "Fundamental diagram estimation through passing rate measurements in congestion," *IEEE Transactions on Intelligent Transportation Systems*, vol. 10, no. 2, pp. 355–359, 2009.

[37] S. Andrews and M. Cops, "Final report: Vehicle infrastructure integration proof of concept executive summary–vehicle," *US DOT, IntelliDrive (sm) Report FHWA-JPO-09-003*, 2009.

[38] X. Huang, S. Mehrkanoon, and J. A. Suykens, "Support vector machines with piecewise linear feature mapping," *Neurocomputing*, vol. 117, pp. 118–127, 2013.

[39] E. Candes and J. Romberg, "l_1-norm magic: recovery of sparse signals via convex programming," Techical Report, Caltech, Tech. Rep., 2005.

[40] M. J. Grace and R. B. Potts, "A theory of the diffusion of traffic platoons," *Operations Research*, vol. 12, no. 2, pp. 255–275, 1964.

[41] F. Qiao, H. Yang, and W. H. Lam, "Intelligent simulation and prediction of traffic flow dispersion," *Transportation Research Part B: Methodological*, vol. 35, no. 9, pp. 843–863, 2001.

[42] D. I. Robertson, "Transyt - a traffic network study tool," *RRL Report, No. LR253, Transport and Road Research Laboratory, Growthorne, UK*, 1969.

[43] P. Hunt, D. Robertson, R. Bretherton, and R. Winton, "Scoot-a traffic responsive method of coordinating signals," Tech. Rep., 1981.

[44] E. Lieberman and A. B.J., "Traflo: A new tool to evaluate transportation system management strategies," *Transportation Research Record*, vol. 772, pp. 9–15, 1980.

[45] M. Grant and S. Boyd, "CVX: Matlab software for disciplined convex programming, version 2.1," http://cvxr.com/cvx, Mar. 2014.

[46] M. Grant and S. Boyd, "Graph implementations for nonsmooth convex programs," *Recent advances in learning and control*, pp. 95–110, 2008.

[47] S.-J. Kim, K. Koh, M. Lustig, S. Boyd, and D. Gorinevsky, "An interior-point method for large-scale-regularized least squares," *IEEE journal of selected topics in signal processing*, vol. 1, no. 4, pp. 606–617, 2007.

[48] R. Florin and S. Olariu, "A survey of vehicular communications for traffic signal optimization," *Vehicular Communications*, vol. 2, no. 2, pp. 70 – 79, 2015.

[49] J. S. Greenfeld, "Matching gps observations to locations on a digital map," in *Transportation Research Board 81st Annual Meeting*, 2002.

[50] F. Caron, E. Duflos, D. Pomorski, and P. Vanheeghe, "Gps/imu data fusion using multisensor kalman filtering: introduction of contextual aspects," *Information fusion*, vol. 7, no. 2, pp. 221–230, 2006.

Monica Menendez received the dual B.S. degree (summa cum laude) in civil and architectural engineering from University of Miami, FL, USA, in 2002 and the M.S. and Ph.D. degrees (focusing on transportation) from University of California, Berkeley, CA, USA, in 2003 and 2006, respectively. Since January 2018, she is an Associate Professor of Civil Engineering at New York University in Abu Dhabi; and a Global Network Associate Professor of Civil and Urban Engineering at the Tandon School of Engineering in New York University. Between 2010 and 2017, she was the Director of the research group Traffic Engineering at ETH Zurich; and prior to that, a Management Consultant at Bain & Company. She has authored or coauthored multiple publications in the areas of transportation, operations research, and construction management. Her research interests include traffic flow theory, modeling, operations, and control, as well as sustainable transportation and logistics.

Kaidi Yang received a B.S. degree in Automation and a dual B.S degree in Mathematics from Tsinghua University, Beijing, China in 2011; an M.S. degree in Control Science and Engineering from Tsinghua University.

Since 2014, he has been a PhD candidate at Swiss Federal Institute of Technology (ETH), Zurich, Switzerland. His main research interest is traffic operations and control with connected and automated vehicles.